

Generate Traveling Acoustic waves on the Surface of Sun and Shadow Plant by Photoacoustic Spectroscopy

Salma A. H .Ali ¹, Mubrarak Dirar Abd-Alla², , Abdalskhi .S.M.Hamed³ & Abdalgadir.Alf.Abdalgadir⁴

¹Sudan University of Science & Technology-College of Science-Department of Physics- Khartoum- Sudan

²International University of Africa –Faculty of Pure and Applied Science- Department of Physics - Khartoum- Sudan

³Al-Neenlen University – Faculty of Science and Technology Department of Physics-
Khartoum- Sudan

⁴Al-Neenlen University – Faculty of Science and Technology Department of Environmental - ;hartoum- Sudan

Abstract: *In this study, used Photoacoustic spectroscopy (PAS) generate traveling acoustic waves on the surface of plant that growth in Sun and Shadow (Bougainvillea spp 11 in shadow, Bougainvillea spp 1 in sun, Citrus Sanseis in sun, Citrus Sanseis in shadow, Canna Indicia in sun, Canna Indicia in shadow, Ixora Coccinnia in sun, Ixora Coccinnia in shadow, Bougainvillea Spp2 in sun, Bougainvillea Spp2 in sun, Citrus Paradisi in shadow and Citrus Paradisi in sun). In this study applied Diodes Laser 450 nm power (4.4) mW. The periodic variation in the strain leads to a periodic variation in the refractive index owing to the photo elastic effect .For all samples generate traveling acoustic waves on the surface of a plant at frequency range (0.014x10¹⁴ and 0.85x10¹⁴) Hz.*

Keywords: Photoacoustic spectroscopy, Diodes Laser , photo elastic effect , plant leaves, growth in sun and `growth in shadow

1. Introduction

Photoacoustic spectroscopy (PAS), sometimes also termed optoacoustic spectroscopy, is used to study energy emission resulting from nonradioactive de-excitation following absorption of radiation. Several reviews have already been published on the method in general [1,2] and its application in biology [3,4,5] . The detection of the photoacoustic effect dates back to experiments of Alexander Graham Bell [6], John Tyndall, Wilhelm Röntgen and Lord Rayleigh in 1880. For the history of PAS see [7] . It was not until 1973 that photoacoustic spectroscopy started to be used in a wide range of different applications. This "rediscovered" technique provides the following main advantages over the conventional types of spectroscopy. It allows the characterization and analysis of substances in highly light-scattering and opaque materials such as powders (drugs, insulators, \and metals), amorphous solids (glasses), gels (films), suspensions (bacteria, algae, cell organelles) and tissues (leaves, skin). Non-destructive and in vivo studies at different subsurface levels of a material (depth profile analysis), studies of the optical and energy properties of the sample, gathering information about the de-excitation states of molecules (e.g. energy state, quantum yield) and about the lifetime of the intermediates of chemical reactions.

These major advantages make PAS particularly suitable for studying biological material in vivo. In plant material PAS has been used since 1976 for the spectroscopic characterization and detection of pigments in phytoplankton [8] and tissues or cell layers including depth profile analysis [9,10] . PAS was used for measuring photosynthetic activity by comparing the heat emission of active and inactive sample [11]. PAS in combination with other types of spectroscopy (e.g. fluorescence and absorption) and gas exchange studies seems to be a valuable tool to clarify a variety of questions in today's photosynthesis research. Principle of the photoacoustic effect: Non-radiative de-excitation processes in a sample cause energy emission. If the sample is excited by absorption of intermittent (modulated) light energy pulses are emitted with the same modulation frequency as that of the incident excitation light. These energy pulses create changes in the construction of sample and can thus be detected as an acoustic signal. Only a small number of photoacoustic spectrometers are commercially available. Most of the results presented up to now were achieved with "homemade" apparatus. For excitation one may use a strong conventional light source e.g. incandescent arc lamps or a laser. Excitation wavelength is selected and scanned by means of a monochromator in the spectral range of the ultraviolet, visible and near infrared. The light beam falling upon the sample is periodically interrupted (modulated), e.g. by a rotating sector (chopper). The modulation frequency can be varied within a given range, normally between 1 Hertz and several Kilohertz (acoustic frequency). Parameters determining the strength of the photoacoustic signal (optimum signal/noise ratio) The height of the photoacoustic signal is determined by the characteristics of the spectrometer and of the sample [10,11] . To receive a high signal/ noise ratio the following parameters are of importance: instrumentation: high photon flux of the excitation light with precautions concerning photodestruction of the samples . appropriate modulation frequency, normally between 5 Hz to 500 Hz . low temperature thin gas layer above the sample sample: high light absorption of the sample . high quantum yield for non-radiative de-excitation of the sample . low thermal conductivity of samples with high light absorption . high thermal conductivity of optically more transparent samples (with lower light absorption) . . large sample surface (to allow a good thermal transfer from sample into the gas phase of the sample compartment)[12].

Acousto-Optic Modulator , An induced strain (S) in a crystal changes its refractive index n . This is called the photoelastic effect. We can generate traveling acoustic waves on the surface of a plant samples by attaching interdigitated electrodes and applying a

modulating Laser at frequencies. The applied Laser field generates a strain in the plant samples. The periodic variation in the strain leads to a periodic variation in the refractive index owing to the photoelastic effect. We can simplistically view the piezoelectric crystal surface region as Bragg diffraction equation $n\lambda = d \sin\theta$. The acoustic wave and thus the diffraction pattern moves on the plant samples surface. As a result of the Doppler effect, the diffracted light beam has either a slightly higher or slightly lower frequency depending on the direction of the traveling acoustic wave. When the acoustic wave is traveling towards the incoming optical beam, then the diffracted optical beam frequency is upshifted[13].

Experimental Arrangement

As the photoacoustic and related photo thermal phenomena comprise a large diversity of facets, there exist a various detection technique which rely on the acoustic or thermal disturbances caused by the absorbed radiation, the selection of the most appropriate scheme for a given application depends on the sample, the sensitivity to be achieved, ease of operation, ruggedness, and any requirement and any require for non-contact detection. Experimental schemes for photoacoustic studies on solid sample includes the measurement of the generated vibration bonds wave either directly in the sample with a piezoelectric sensor for the pulsed regime, or indirectly in the USB 2000 spectrometer which is in contact with the sample by a computer as show in fig (1).

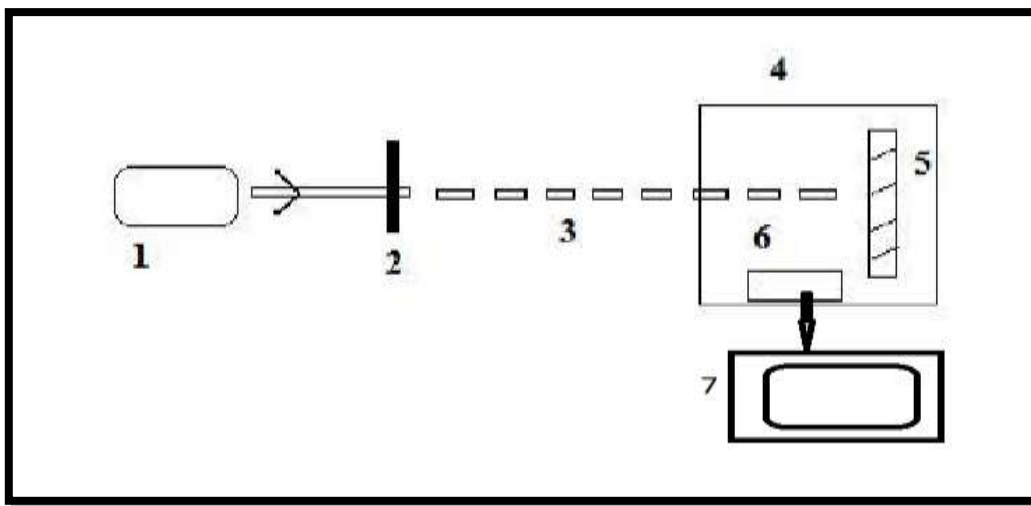


Fig (1) typical experimental arrangements used for Photoacoustic spectroscopy. (1) Light source (2) the chopper (3) chopped light (4) photoacoustic cell (5) sample (6) USB-2000 spectrometer (detection sensors) (7) computer

Results:

After arrangement the experimental generate traveling acoustic waves on the surface of some plant that growth in sun and shadow by the Photoacoustic spectroscopy as showing in the results blow.

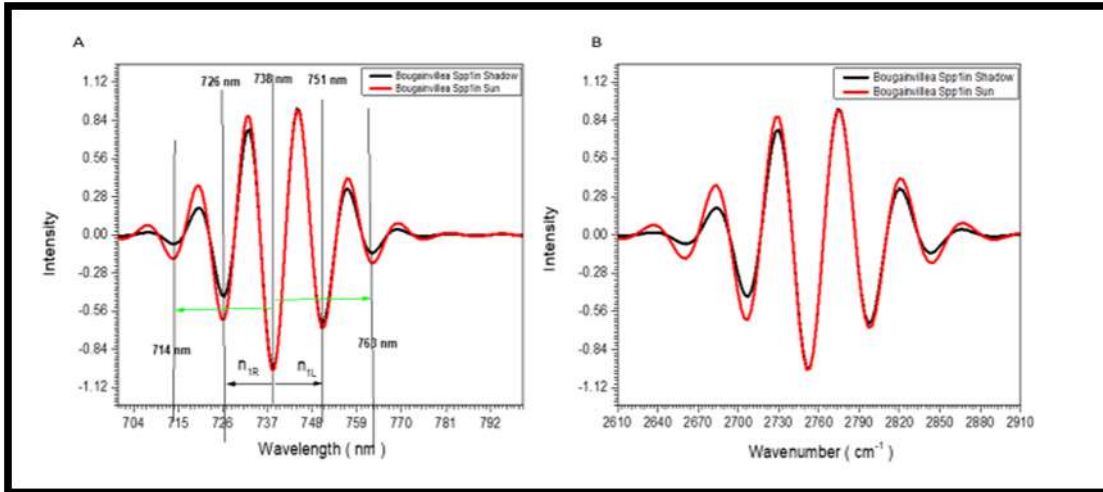


Fig (2) the experimental acousto-optic Modulators of Bougainvillea Spp1 samples growth in sun and shadow ,(A) Bragg regime, (B) The frequency of acoustic optic modulation

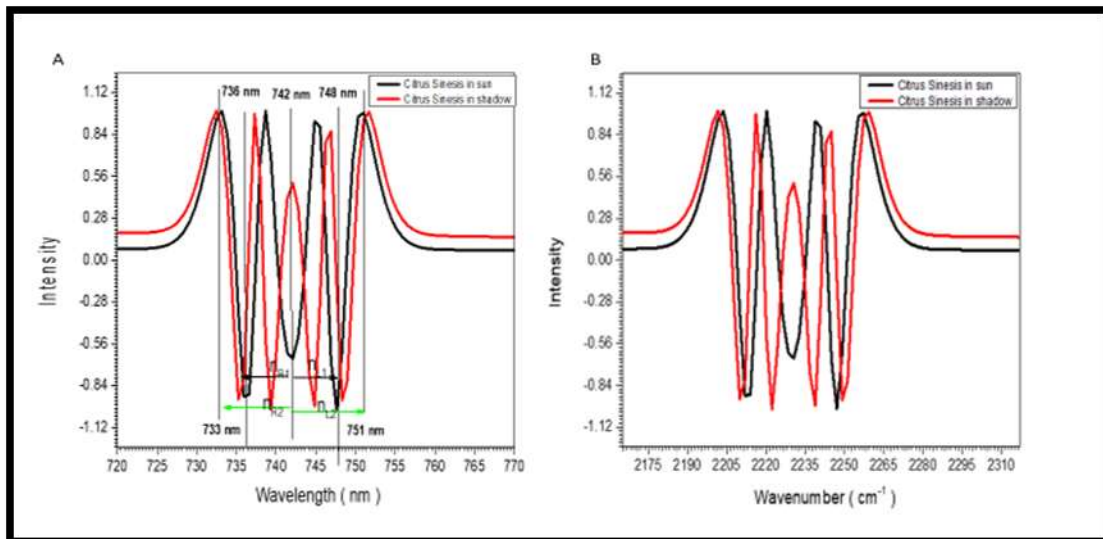


Fig (3) the experimental acousto-optic Modulators of Citrus Sinesis samples growth in sun and shadow ,(A) Bragg regime ,(B) The frequency of acoustic optic modulation

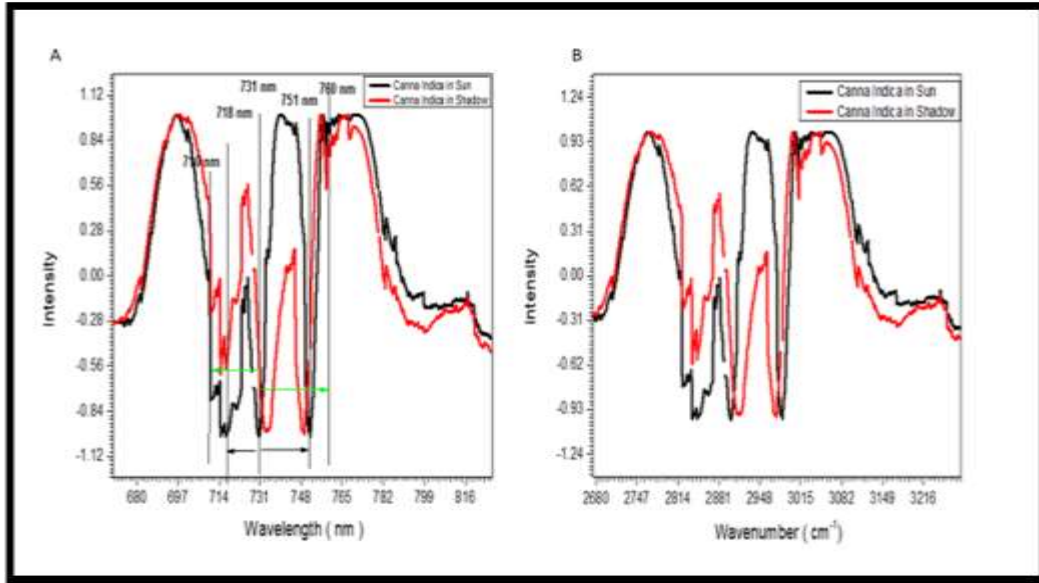


Fig (4) the experimental acousto-optic Modulators of Canna Indica samples growth in sun and shadow , (A) Bragg regime ,(B) The frequency of acoustic optic modulation

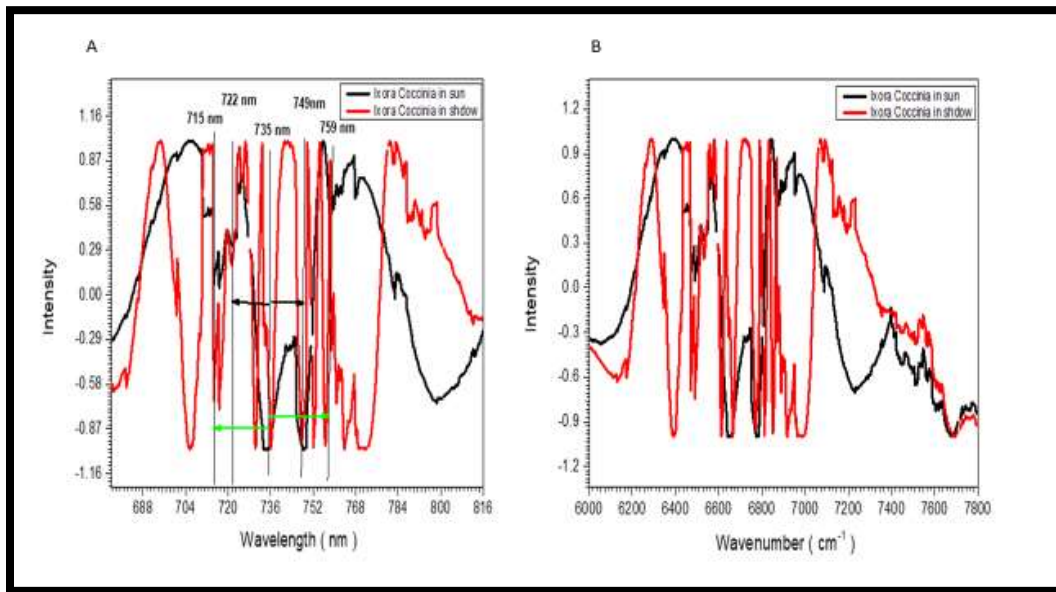


Fig (5) the experimental acousto-optic Modulators of Ixora Coccinia samples growth in sun and shadow ,(A) Bragg regime ,(B) The frequency of acoustic optic modulation

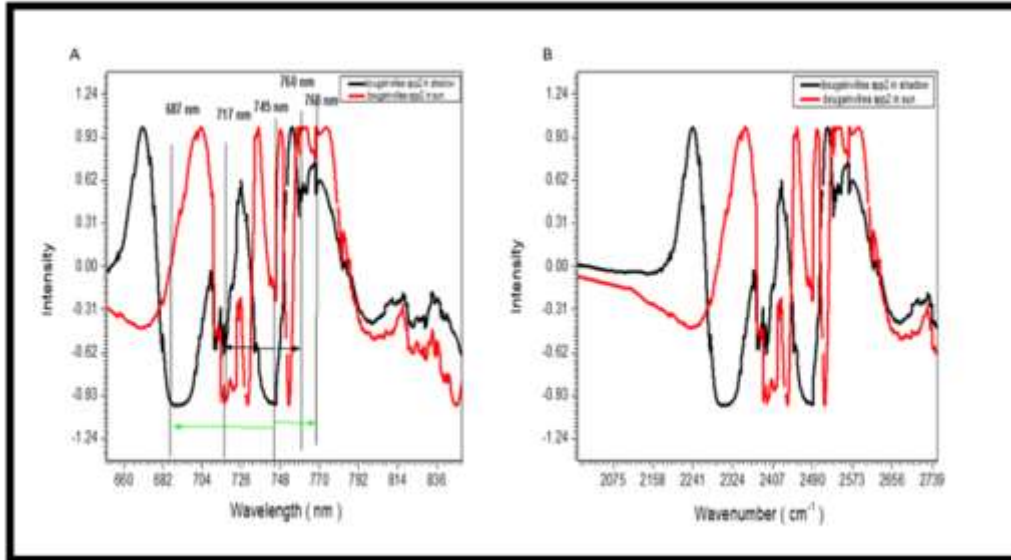


Fig (6) the experimental acousto-optic Modulators of Bougainvillea Spp2 samples growth in sun and shadow, (A) Bragg regime ,(B) The frequency of acoustic optic modulation

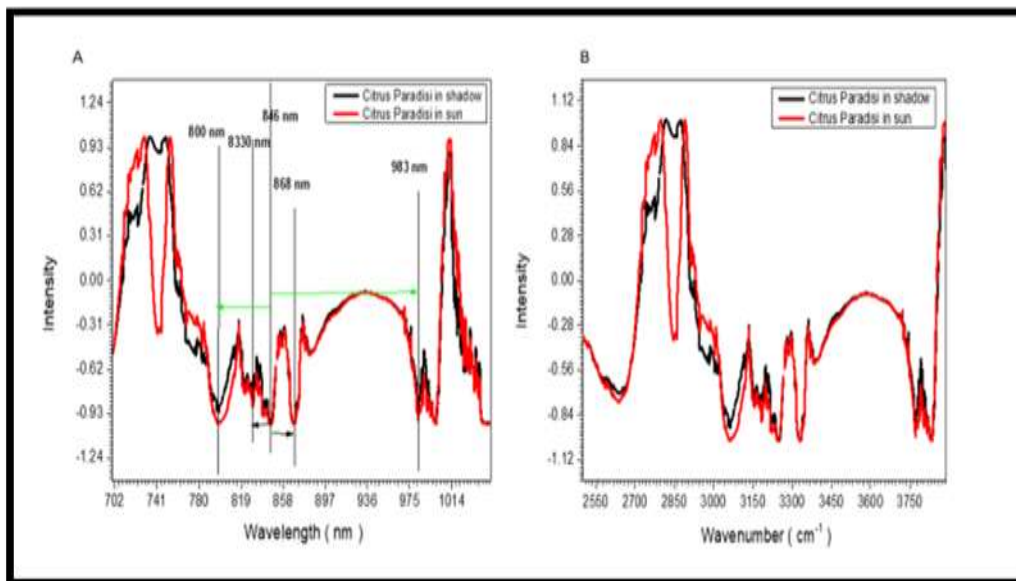


Fig (7) the experimental acousto-optic Modulators of Citrus Paradisi samples growth in sun and shadow , (A) Bragg regime ,(B) The frequency of acoustic optic modulation

Table (1) show the samples and the order diffraction of bragg regime

No	samples	Order Diffraction of Bragg Regime (nm)					
		$n_{L=2}$	$n_{L=1}$	$n_{R=1}$	$n_{R=2}$	\bar{n}_1	\bar{n}_2
1	Bougainvillea spp 11 in shadow	12	6	6	12	6	12
2	Bougainvillea spp 1 in sun	11	5	7	13	6	12
3	Citrus Sanseis in sun	9	6	6	9	6	9
4	Citrus Sanseis in shadow	8	7	5	10	6	9
5	Canna Indicia in sun	29	20	13	21	16.5	25
6	Canna Indicia in shadow	30	19	14	20	16.5	25
7	Ixora Coccinnia in sun	24	14	13	20	13.5	22
8	Ixora Coccinnia in shadow	23	15	12	21	13.5	22
9	Bougainvillea Spp2 in shadow	23	15	28	42	21.5	35.5
10	Bougainvillea Spp2 in sun	22	16	27	43	21.5	35.5
11	Citrus Paradisi in shadow	37	22	16	46	19	41.5
12	Citrus Paradisi in sun	36	23	15	47	19	41.5

Discussion

Fig (2) show the experimental acousto-optic Modulators results of Bougainvillea Spp1 samples growth in sun and shadow ,(A) Bragg regime, (B) The frequency of acoustic optic modulation . In fig (2) (A) show that the main wavelength of bragg regime modal at 738nm, the first order diffraction left at (751) nm and first right at (726) nm. The second order diffraction left at (763) nm, and second right at (714) nm. And in fig(2) (B) showing the curve of relation between wavenumber and the intensity of acoustic optic modulation that calculated by Bragg regime of Bougainvillea Spp1 growth in sun and shadow ,and the frequency of acoustic optic modulation at the first average order equal (0.05×10^{14} Hz) and the second average order equal (0.025×10^{14} Hz) . The average wavenumber of acoustic optic wave of samples Bougainvillea Spp1 growth in sun and shadow equal 46 cm^{-1} . In fig (3) show the experimental acousto-optic Modulators results of Citrus Sinesis samples growth in sun and shadow, (A) Bragg regime, (B) The frequency of acoustic optic modulation. In fig(3) (A) show the bragg regime of Citrus Sinesis samples growth in sun and shadow was applied .The main wavelength of bragg regime at 742nm, the first order diffraction left at (748) nm and first right at (736)nm. The second order diffraction left at (751) nm, and second right at (733) nm. In fig(3) (B) showing the curve of relation between wavenumber and the intensity of acoustic optic modulation that made from Bragg regime of Citrus Sinesis growth in sun and shadow, and the average frequency of acoustic optic modulation at the first order equal (0.05×10^{14} Hz) and the second average order equal (0.033×10^{16} Hz). The average wavenumber of acoustic optic wave of samples Bougainvillea Spp1 growth in sun and shadow equal 17 cm^{-1} . In fig (4) the experimental acousto-optic Modulators of Canna Indica samples growth in sun and shadow , (A) Bragg regime ,(B) The frequency of acoustic optic modulation , the main wavelength of bragg regime modal at 731 nm, the first order diffraction left at (751) nm and first right at (718) nm, and the second order diffraction left at (700) nm ,and second right at (710) nm as show in fig (4) (A). In fig(4) (B) showing curve relation between wavenumber and the intensity of acoustic optic modulation that calculated by Bragg regime , and the average frequency of acoustic optic modulation at the first order equal (0.0182×10^{14} Hz) and the second average order equal (0.012×10^{14} Hz) . The average wavenumber of acoustic optic wave of samples Canna Indica growth in sun and same plant in shadow equal (115 cm^{-1}). In fig (5) show the experimental acousto-optic Modulators results of Ixora Coccinia samples growth in sun and shadow ,(A) Bragg regime ,(B) The frequency of acoustic optic modulation ,the main wavelength of bragg regime modal at 735nm, the first order diffraction left at (749) nm and first right at (722)nm. The second order diffraction left at (759) nm, and second right at (715) nm. In fig (5) (B) showing the curve of relation between wavenumber and the intensity of acoustic optic modulation that calculated by Bragg regime, the frequency average for the first order equal (0.022×10^{14} Hz) and the second average order equal (0.014×10^{14} Hz) . The average frequency of acoustic optic wave of samples Ixora Coccinia growth in sun and shadow equal (290 cm^{-1}). In fig (6) the experimental acousto-optic Modulators of Bougainvillea Spp2 samples growth in sun and shadow, (A) Bragg regime ,(B) The frequency of acoustic optic modulation , the main wavelength of bragg regime modal at 745 nm, the first order diffraction left at (760) nm and first right at (717)nm. The second order diffraction left at (768) nm, and second right at (687) nm. In fig (6) (B) showing the curve of relation between wavenumber and the intensity of acoustic optic modulation that calculated by Bragg regime of Bougainvillea Spp2 growth in sun and shadow. Moreover, the average frequency of acoustic optic modulation of the first order equal (0.0139×10^{14} Hz) and the second order equal (0.85×10^{14} Hz). The average wavenumber of acoustic optic wave of Bougainvillea Spp2 growth in sun and shadow equal 127 cm^{-1} . At Last for fig (7) show the experimental acousto-optic Modulators results of Citrus Paradisi samples growth in sun and shadow , (A) Bragg regime ,(B) The frequency of acoustic optic modulation ,the main wavelength of Bragg regime modal at 846 nm, the first order diffraction

left at (868) nm and first right at (830)nm. The second order diffraction left at (983) nm, and second right at (800) nm. In fig(7) (B) showing the relation between wavenumber and the intensity of acoustic optic modulation that calculated by Bragg regime of Citrus Paradisi growth in sun and shadow, the average frequency of acoustic optic modulation for the first order equal $(0.0158 \times 10^{14} \text{ Hz})$ and the second order equal $(0.723 \times 10^{14} \text{ Hz})$. The average wavenumber of acoustic optic wave of Citrus Paradisi growth in sun and shadow equal 77 cm^{-1} . The reason of different frequency between the sun and shadow plant come from the concentration of components, which consist of the plant leaves, as showing in table (1).

Conclusions

Acoustic optic modulation that generated from leaves of plant growth in sun and shadow in different frequency and wavenumber, the reason of frequency and wavenumber come from the concentration of components, which consist of the plant leaves.

References

- [1] Wang SQ, Xiang LZ, Liu YT, Liu H (2018) Photo-acoustic based non-contact and non-destructive evaluation for detection of damage precursors in composites. In: Abstracts of ASME 2018 international mechanical engineering congress and exposition, ASME, Pittsburgh, 9–15 November 2018. <https://doi.org/10.1115/IMECE2018-86148>
- [2] Wang SQ, Tran T, Xiang LZ, Liu YT (2019) Non-destructive evaluation of composite and metallic structures using photo-acoustic method. In: Abstracts of AIAA scitech 2019 forum, AIAA, San Diego, 7–11 January 2019. <https://doi.org/10.2514/6.2019-2042>
- [3] Liu HH, Zhao YB, Bo SH, Chen SL (2020) Application of photoacoustic imaging for lithium metal batteries. In: Abstracts of SPIE, SPIE, Online Only, 10 October 2020. <https://doi.org/10.1117/12.2575184>
- [4] Du C, Twumasi JO, Tang QX, Guo X, Zhou JC, Yu T et al (2018) All-optical photoacoustic sensors for steel rebar corrosion monitoring. *Sensors* 18(5):1353. <https://doi.org/10.3390/s18051353>
- [5] Lu QB, Liu T, Ding L, Lu MH, Zhu J, Chen YF (2020) Probing the spatial impulse response of ultrahigh-frequency ultrasonic transducers with photoacoustic waves. *Phys Rev Appl* 14(3):034026. <https://doi.org/10.1103/PhysRevApplied.14.034026>
- [6] Chen SL (2017) Review of laser-generated ultrasound transmitters and their applications to all-optical ultrasound transducers and imaging. *Appl Sci* 7(1):25. <https://doi.org/10.3390/app7010025>
- [7] Guggenheim JA, Li J, Allen TJ, Colchester RJ, Noimark S, Ogunlade O et al (2017) Ultrasensitive plano-concave optical microresonators for ultrasound sensing. *Nat Photon* 11(11):714–719. <https://doi.org/10.1038/s41566-017-0027-x>
- [8] Hosseinaee Z, Le M, Bell K, Reza PH (2020) Towards non-contact photoacoustic imaging [review]. *Photoacoustics* 20:100207. <https://doi.org/10.1016/j.pacs.2020.100207>
- [9] Wissmeyer G, Pleitez MA, Rosenthal A, Ntziachristos V (2018) Looking at sound: optoacoustics with all-optical ultrasound detection. *Light Sci Appl* 7 <https://doi.org/10.1038/s41377-018-0036-7>
- [10] Schellenberg MW, Hunt HK (2018) Hand-held optoacoustic imaging: a review. *Photoacoustics* 11:14–27. <https://doi.org/10.1016/j.pacs.2018.07.001>
- [11] Attia ABE, Balasundaram G, Moothanchery M, Dinish US, Bi RZ, Ntziachristos V et al (2019) A review of clinical photoacoustic imaging: current and future trends. *Photoacoustics* 16:100144. <https://doi.org/10.1016/j.pacs.2019.100144>
- [12] Sung-Liang Chen^{1,2,3*} and Chao Tian⁴- Recent developments in photoacoustic imaging and sensing for nondestructive testing and evaluation - Chen and Tian *Visual Computing for Industry, Biomedicine, and Art* (2021) 4:6 <https://doi.org/10.1186/s42492-021-00073-1>
- [13] S. O. Kasap, “Optoelectronics and Photonics: Principles and Practices”, Prentice Hall, Upper Saddle River, NJ 07458, 2001, Chapter 7, “Polarization and modulation of light”.